Crystalline Forms of 4,4'-Methylenediantipyrine: Crystallographic Unit Cell for the Anhydrous Form, from Laboratory Powder XRD Pattern by DASH Program Package

Dorottya Fruzsina Bánhegyi[1*], János Madarász[2**], Elemér Fogassy[1], Emese Pálovics[1], György Pokol[2]

[1] Department of Organic Chemistry and Technology, Faculty of Chemical Technology and Biotechnology, Budapest University of Technology and Economics, Műegyetem rkp. 3, H-1111 Budapest, Hungary
[2] Department of Inorganic and Analytical Chemistry, Faculty of Chemical Technology and Biotechnology, Budapest University of Technology and Economics, Műegyetem rkp. 3, H-1111 Budapest, Hungary
* Corresponding author, e-mail: banhegyi.dorottya.fruzsina@vbk.bme.hu
**Corresponding author, e-mail: madarasz.janos@vbk.bme.hu

Abstract

Crystalline unit cell structure of anhydrous title compound, diantipyrinylmethane (CAS Registry No. 1251-85-0), a substance usually obtained as a by-product in Mannich type reactions of antipyrine, has been modelled by the help of powder X-ray diffraction, applying the DASH software package and crystal coordinates coming from former single crystal X-ray structure determinations (CSD codes FADDIY and FADDIY01) of its monohydrate. The unit cell of the anhydrate compound belongs to the monoclinic space group $P2_1/a$, with unit cell parameters of $a = 14.604$, $b = 9.858$, $c = 14.509$ Å, $\beta = 95.56$ °, $V = 2078.9$ Å^3, $Z = 4$, $Z' = 1$. Comparisons of FT-IR spectrum and thermal behavior of the anhydrous and monohydrated forms confirm differences in degree of hydration and solid state structure, while those of ^{1}H- and ^{13}C NMR-spectra show their molecular identity.

Keywords

1 Introduction

Most crystal and molecule structure determinations carried out by X-ray diffraction are based on successful growth of a single crystal of organic compounds [1, 2]. In case, when single crystal growth fails, powder X-ray diffraction still provides a little hope to extract some structural information [3]. Luckily, several software programs have been compiled till now to help the efforts for structural determinations from powder data [4, 5], aiming at various organic compounds, especially pharmaceuticals. Among them, the DASH software package [6] is a versatile, user-friendly graphical-user-interface-driven computer program, which earlier was distributed together with Cambridge Structural Database System [7] package, and now it available separately and publicly at world wide web (link to 'github.com/ccdc-opensource/dash/releases'), as well. It serves continuously quite well [8, 9] on powder diffraction data collected in high resolution by synchrotron radiation [10], including e.g., mebendazole Form A [11]. Laboratory pattern collections were also tested by the DASH package [12]. Several structures, obtained successfully with the help of the DASH program, are also reported for various crystalline pigments [13, 14] and recently for (*RS*)-trichlormethiazide [15], when their diffraction patterns were measured only by laboratory X-ray tubes. Anhydrates of ezetimibe [16], morphine [17], naloxone hydrochloride and naltrexone hydrochloride [18] were also determined from laboratory powder diffraction data by application of DASH, where the initial molecular geometries were taken from the single-crystal structure of the monohydrates by excluding the water molecule. Similarly to the latter cases, we could find our title compound in an anhydrous form, and tried to resolve its unknown unit cell features as deep as possible, based on its laboratory powder pattern and known monohydrate structure, applying

build-in indexing and simulated annealing opportunities of the DASH program package [6].

There are several indications for the existence of diantipyrinylmethane (or 4,4'-methylenediantipyrine, CAS Registry No. 1251-85-0, see structure in Table 1), obtained usually as a by-product of Mannich-type reactions of antipyrine, as a solid compound in at least two crystalline forms, especially either in anhydrous or monohydrate forms. The melting point of 4,4'-methylenediantipyrine is mostly observed in the range of 176–181 °C [19–24], but exceptionally it is also reported even at 153–154 °C [25]. Actually, two single crystal structural determinations are available in the Cambridge Structural Database (CSD, CCDC) [1, 7], both are for the monohydrate form of 4,4'-methylene-diantipyrine, with structural codes FADDIY [26] and FADDIY01 [27], which were measured at −70 and ca. +20 °C, respectively, and both of them indicate a space group symmetry of P2$_1$/c and closely related unit cell structures. Nevertheless, there are several various powder XRD patterns of 'low precision' (i.e., which are without assignation of crystal system or unit cell information) but only for anhydrous forms of the title compound in the international PDF4+ database (ICDD) [28]. Among them, the PDF File No. 00-021-1604 (unindexed pattern, deposited in 1967, in frame of a ICDD Grant-in-aid support, available by subscription) seems to be the most reliable one.

We have been lucky to obtain and study both anhydrous and monohydrate forms of diantipyrinylmethane, and tried to index their room temperature powder patterns measured by laboratory X-ray tube and establish the still missing conventional crystallographic unit cell parameters of the anhydrous form by the help of DASH software package [6].

2 Experimental
2.1 Synthesis of anhydrous 4,4'-methylenediantipyrine
0.36 mL formaldehyde (as a 35% aqueous solution) and 0.28 mL cc. HCl in 2 mL of water was added to 2.6 mmol (0.5 g) racemic antipyrine and refluxed for 24 hours. After completion of the reaction, the mixture was extracted with 15 mL of dichloromethane. After separating the phases, 1.5 ml 30% V/V% KOH/aq was added to the aqueous phase. The opal solution obtained was extracted by 15 mL of dichloromethane. The organic phase was dried over Na$_2$SO$_4$. The obtained product was crystallized from diethyl ether. Recrystallization from aqueous ethanol resulted in monohydrate form.

2.2 Powder X-ray Diffraction (XRD)
Powder XRD patterns were recorded with an X'pert Pro MPD (PANalytical B.v., The Netherlands) multipurpose X-ray diffractometer using Cu Kα radiation ($\lambda = 1.5406$ Å) with Ni filter, X'celerator detector, and "zero background" single crystal silicon or "top-loaded" sample holders in the range of 2θ = 4 − 44°. The X-ray tube was operating at 40 kV and 30 mA.

2.3 Indexing, space group determination and structure modelling based on powder XRD pattern by DASH program package
For special purposes of the simulated annealing method of structural modelling in the DASH software package [6], a step size of 0.0167° up to 2θ = 52° was applied, in order to see the merit of fitting of simulated patterns at high degrees, as well. In this case, the overall measurement time was 39 min. Unit cell searches were carried out by using build-in and external indexing facility (DICVOL91 or later versions [29]) of the DASH program package [6]. Space group determination was also helped by an interfaced program *Extinction Symbol*, a special program that identifies the most probable space groups for a set of reflections and their intensities [30].

2.4 FT-IR and NMR spectroscopies
Fourier transform infrared spectra of the solid powdered samples were measured by PE System 2000 (Perkin Elmer) FTIR spectrophotometer in KBr between 500 and 4000 cm^{-1}.

^{1}H-, ^{13}C-NMR and DEPTQ spectra of the synthesized sample have been measured in CDCl$_3$, in a Bruker Advance 500 NMR Spectrometer (Bruker). Chemical shifts are calculated to tetramethylsilane (TMS).

2.5 Differential Scanning Calorimetry (DSC)
DSC measurements were performed in a DSC 2920 device (TA Instruments Inc., New Castle, DE USA). The powdered samples (3.5-4 mg) were measured in hermetically sealed Al pans at a heating rate of 10 K/min. Pure In metal piece was applied for calibration of temperature and enthalpy, meanwhile an empty sealed pan as reference.

2.6 Thermogravimetry
A simultaneous TG/DTA apparatus (STD 2960 Simultaneous DTA-TGA, TA Instruments Inc., USA), a heating

rate of 10 °C min^{-1}, an air flow rate of 130 mL/min, open Pt crucible was applied.

3 Results and discussion

3.1 XRD Phase identification of anhydrous and monohydrated forms of 4,4'-methylenediantipyrine

This product formed finally from diethyl ether in its anhydrous form and identified by help of the international PDF4+ powder X-ray diffraction database [28], as 4,4-diantipirinylmethane (reference pattern is PDF-00-021-1604, 'unindexed', based on reference sample from British Drug Houses, Ltd., Poole, England, ICDD Grant-in-aid, 1967, Institute of Physics, University College, Wales).

Then a part of the anhydrous sample has also been converted/recrystallized with ethanol to its monohydrate form, for which reference powder XRD patterns are generated from the atomic coordinates of the corresponding single crystal determinations (CSD code of FADDIY and FADDIY01) of 4,4'-methylenediantipyrine monohydrate [26, 27], see Fig. 1.

3.2 Analytical identification of molecule of 4,4'-methylenediantipyrine (diantipyrinylmethane)

The chemical constitutional formulae is confirmed both by ^{1}H- and ^{13}C-NMR(DEPTQ) spectra (CDCl$_3$, 500 MHz), which are found (Table 1) in harmony with the symmetry of molecular structure and the publicly available spectral references of AIST [31], SciFinder^n [32]).

3.3 Comparison of FTIR spectrum of anhydrous and monohydrated forms

The FT-IR spectrum of both the anhydrous and monohydrated diantipyrinylmethane sample of ours is shown in Fig. 2. IR spectra of the monohydrate form are available in the public databases (AIST [31], SciFinder^n [32]). These references are in good agreement with the spectrum obtained for our monohydrate sample. Anyhow, the spectrum of anhydrous sample indicates – in the regions of 3100–3800 cm^{-1} – an absence of water of crystallization or hydration, and lack of hydrogen bonds, compared to broad bands of monohydrate, originating from widening of νOH stretching vibrations. The vibrational bands below 1800 cm^{-1} reflect both strong similarities and small but significant differences in molecular vibration frequencies, as well. The mall differences indicate or confirm slight but significant alterations of force fields of secondary interactions in the solid anhydrous vs. monohydrated forms.
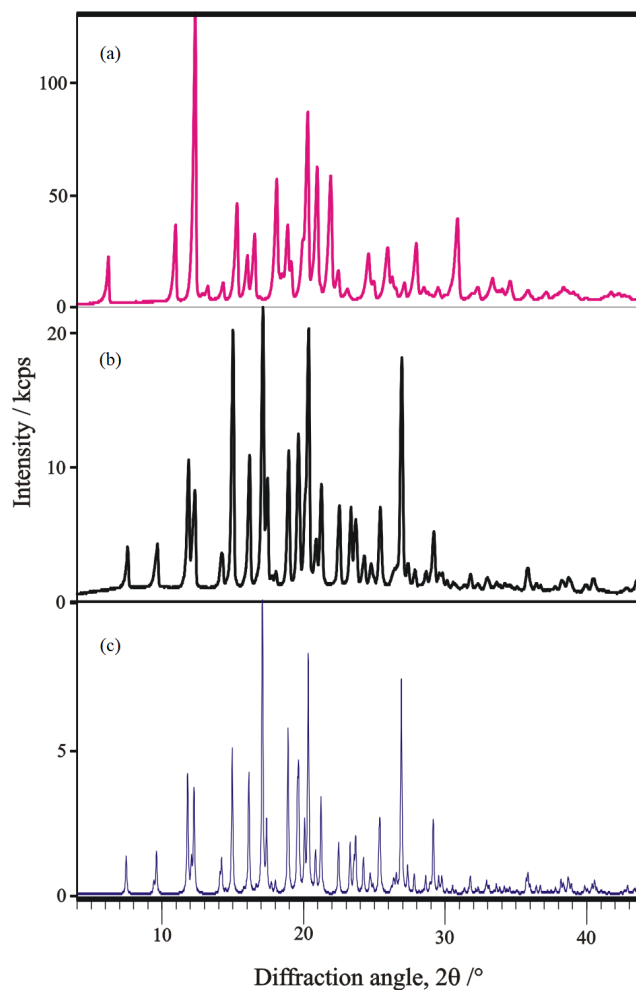
Fig. 1 XRD profile of (a) anhydrous 4,4'-methylenediantipyrine, product from diethyl ether, Et$_2$O, corresponding to PDF-00-021-1604; (b) 4,4'-methylenediantipyrine monohydrate obtained from ethanol, EtOH; (c) 4,4'-methylenediantipyrine monohydrate reference pattern (calculated, FADDIY01, [27]), in comparison

3.4 Comparison of thermal behavior of anhydrous and monohydrated forms

DSC curves, measured on both anhydrous and monohydrated form in sealed Al crucible, are exhibited in Fig. 3(a). Our monohydrate sample shows an endothermic dehydration effect at around 156–158 °C [25, 27] and a final melting point ranging from 177 to 179 °C. The latter range is close to those given for the corresponding anhydrous compound in the former special literature [19–24]. Thermogravimetric weight loss till 174 °C clearly indicates the release of one molecule of water from the sample with monohydrate formulae, measured as ca. 4.55% (Fig. 3(b), theoretical mass loss because of dehydration calculated for $C_{23}H_{24}N_4O_2 \cdot H_2O$ is 4.43%). Limited weight changes, probably because of sublimation of the anhydrous compound, can be considered

Table 1 Readouts and assignations of ^{1}H- and ^{13}C-NMR chemical shifts (CDCl$_3$) of 4,4'-methylenediantipyrine, in comparison with reference data of AIST [31]

	^{1}H NMR (500 MHz, CDCl$_3$) δ, ppm	^{1}H NMR (400 MHz, CDCl$_3$) δ, ppm (AIST, SDBS No. 15285HSP-48-779 [31])
	A: 7.405, A':7.395, B':7.391, B: 7.375 (8H); C: 7.216 (2H); D: 3.256 (s, 2H) E: 2.979 (s, 6H) F: 2.433 (s, 6H)	A: 7.417 B: 7.382 C: 7.234 D: 3.271 E: 2.988 F: 2.441
	s singlet; d doublet; t triplet;	

	^{13}C NMR (125.75 MHz, CDCl$_3$) δ, ppm (DEPTQ)	^{13}C NMR (25.16 MHz, CDCl$_3$) δ, ppm (AIST, SDBS No. 15285CDS-12-482 [31])
	166.21 154.44 135.48 129.06 126.05 123.68 108.50 35.960 15.820 11.492	166.19 154.44 135.45 129.01 126.06 123.67 108.43 35.87 15.73 11.41
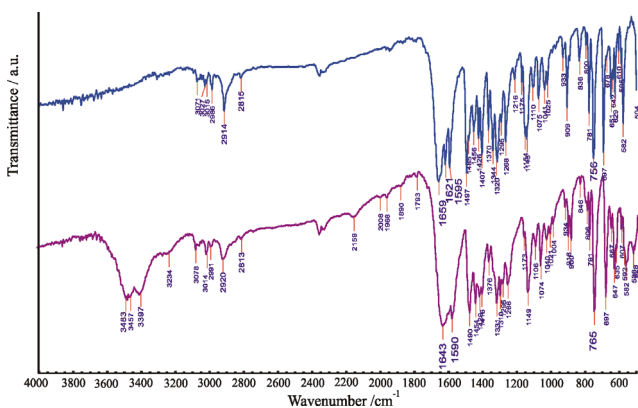
Fig. 2 FT-IR spectrum of our anhydrous 4,4'-methylenediantipyrine (top, from Et$_2$O) and monohydrate sample obtained from EtOH (bottom), in comparison
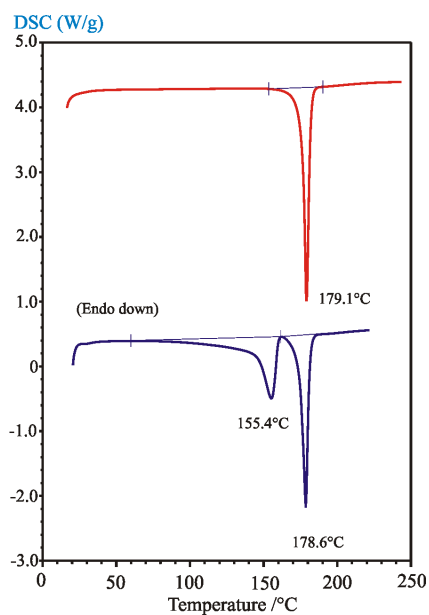
(a)
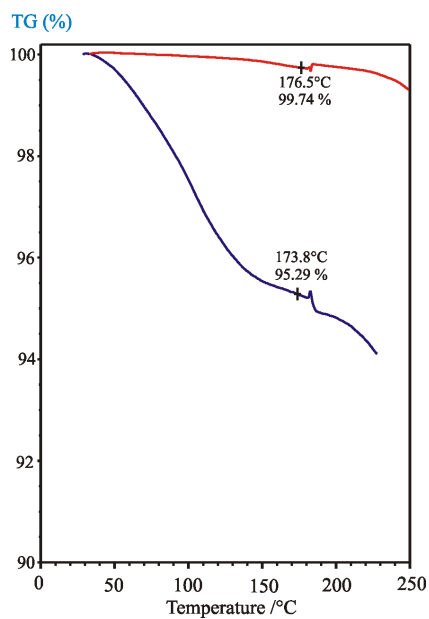
(b)

Fig. 3 Comparison of (a) both DSC heat effects (measured in sealed Al crucibles); and (b) both TG mass losses (obtained in open Pt crucibles) of anhydrous (top curves, in red) and monohydrate 4,4'-methylenediantipyrine sample from EtOH + H$_2$O (bottom curves, in blue) of ours. (Peak temperatures of fusion are reported as melting points)

as negligible till 177 °C. (Small effects such as 'up & down' jumps on the TG curves – during the fusion phenomenon – might come from the high sensitivity of our TG balance being able to sense a kind of 'tropism' or 'taxis' of liquid drops forming within the TG-crucible). The measured main heat effects are 93.36, 83.10, and 96.34 J/g for dehydration, fusion of in situ formed, and of the originally anhydrous

matter, respectively. Unfortunately, no literature values on enthalpies of the dehydration and melting are available for the monohydrate compound.

3.5 Estimation of crystallographic unit cell for the anhydrous and monohydrate forms, from room temperature laboratory powder XRD patterns (by help of the DASH software package)

Based on the anhydrous and monohydrated sample's powder XRD profile measured at room temperature by our laboratory X-ray tube, we have carried out some modelling trials on crystal structures, what has not been reported yet (Table 2). For the anhydrous form, a monoclinic unit cell with space group symmetry $P2_1/a$ (s.g., No. 14) has been found the most appropriate by estimation of expected molecular volume and evaluation of results provided by the interfaced *Extinction Symbol* program [30], and systematic absences, among the cell suggestions obtained with build-in and external indexing facility (DICVOL91 or later program versions [29]) of the DASH program package [6]. The estimated unit cell parameters are summarized in Table 2. Final profile fitting result and molecular content of the unit cell, what could be achieved with the trials of simulated annealing method built in the same DASH program package [6] are shown in Fig. 4. (Corresponding set of atomic coordinates, in the form of crystallographic information file is attached as supplementary information or available on request from the authors.)

A skeleton of formerly solved structures of the corresponding monohydrate form (CSD code FADDIY [26] and FADDIY01 [27]), with known bond distances and angles could be applied as a model for simulations on torsion angles. Although, both solved single crystal structures of monohydrate in CSD database (FADDIY [26]) and FADDIY01 [27]) exhibit hydrogen bonds involving hydrogens of H_2O molecules and carbonyl oxygen atoms of antipyrine molecules, in the case of anhydrous form there is no opportunity for formation of any hydrogen bonds, as it is also reflected in the FT-IR spectrum of the anhydrous form (Fig. 2, top spectrum). The hydrogen bonds in the monohydrate structure of FADDIY01 [27] and a conformational comparison of the molecules in the monohydrate and anhydrous forms are demonstrated in Fig. 5(a) and (b). The conformational differences are purely arising from the different torsional angles occurring in the two forms. More detailed comparisons of secondary interactions, as e.g., in [33] have no worth carrying out in our case, because of the approximate feature of our modelling results.

4 Conclusion

Crystalline unit cell structure of anhydrous title compound, diantipyrinylmethane, not studied either by powder or single crystal XRD previously, have been successfully indexed (Table 2, 2nd column) and visualized from its powder X-ray diffraction pattern, by DASH program package,

Table 2 Unit cell parameters of anhydrous diantipyrinylmethane estimated from the measured powder XRD patterns by powder pattern indexing (Dicvol [29]) using interactive DASH program [6] (shown together with a trial for monohydrate sample and single crystal references for that).

Crystallographic unit cell parameters	4,4'-methylene-diantipyrine anhydrous form (Et₂O), powder pattern-indexing, rt [DASH, this work]	4,4'-methylene-diantipyrine monohydrate, FADDIY [26] T= −70 °C	4,4'-methylene-diantipyrine monohydrate FADDIY01 [27] T = 20 °C	4,4'-methylene-diantipyrine monohydrate sample (EtOH + H₂O), powder pattern-indexing, rt [DASH, this work]
Crystal system	Monoclinic	Monoclinic	Monoclinic	Monoclinic
Space group	P2₁/a (No. 14)	P2₁/c (No. 14)	P2₁/c (No. 14)	P2₁/c (No. 14)
a (Å)	14.604	11.937(3)	11.879(<1)	11.927
b (Å)	9.858	14.740(4)	14.679(<1)	14.741
c (Å)	14.509	12.085 (3)	12.259 (<1)	12.300
α (°)	90	90	90	90
β (°)	95.56	92.44 (<1)	92.89 (<1)	92.92
γ (°)	90	90	90	90
V (Å³)	2078.870	2124.451	2134.905	2159.795
V (formula unit) (Å³)	519.718	531.113	533.726	539.949
Z/Z'	4/1	4/1	4/1	4/1
Zero shift (°)	0.1320	–	–	0.1809
Pawley fitting c^2	52.275	–	–	15
Profile c^2 after SA[1]	178.93	–	–	180.62

[1] For definitions see at world wide web linked to github.com/ccdc-opensource/dash/wiki/FiguresOfMerit [6]

(a)

(b)
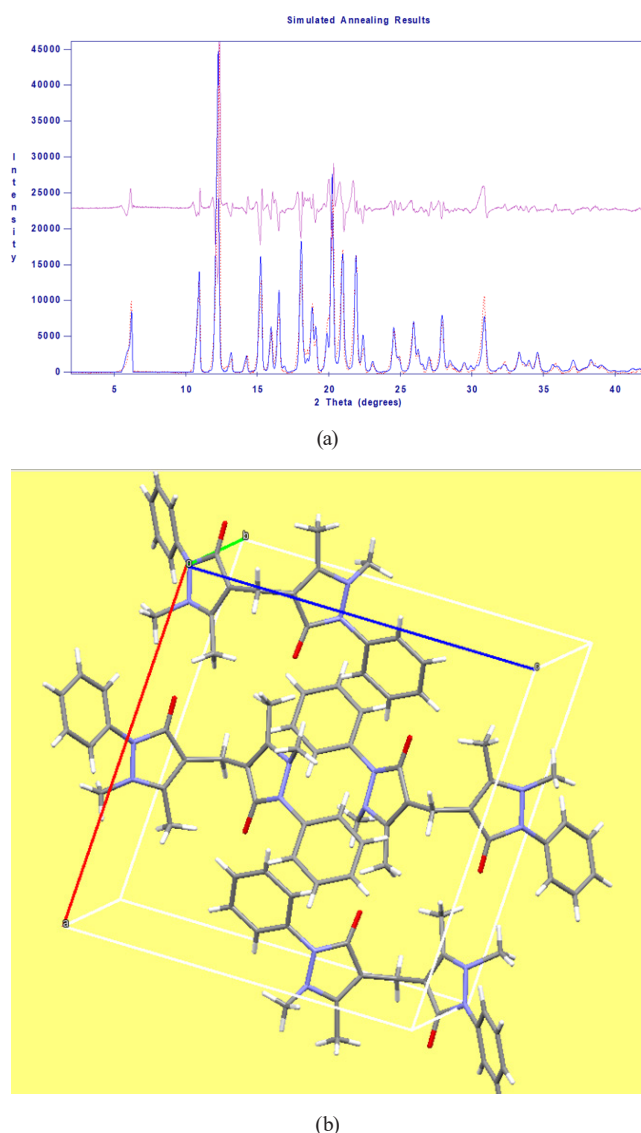
Fig. 4 Final fitting result on XRD profile (a) and unit cell contents (b) of anhydrous diantipyrinylmethane crystalline form, achieved with indexing (DICVOL [29]) and simulated annealing feature of the DASH program package [6]

(a)

(b)

Fig. 5 Arrangements in the crystals: (a) The hydrogen bonds in the monohydrate structure of FADDIY01 [27]; and (b) conformational comparison of the molecules in the monohydrate and anhydrous forms. (The conformational differences are purely arising from the different torsional angles occurring in the two forms)

as this molecule has only 4 torsional rotational degrees of freedom and exists lonely ($Z' = 1$) in the asymmetric unit of its crystalline form (s.g. $P2_1/a$, No. 14, $Z = 4$). Conditions, such as low degree of torsional freedom and presence of only one molecule in the asymmetric cell, increase the opportunity of finding at least an "approximate" structure description based of powder XRD pattern fitting [4, 9, 34] with help of single crystal structural skeleton data obtained previously and available in CSD as rigid body model. Actually, because of the high initial Pawley profile fitting difficulties, arising mainly from usage of a laboratory X-ray tube radiation and of reflection plate sample holder system [35], the precise unit cell structure could not be achieved, it should further be validated from single crystal

growth and XRD structure resolution, but unfortunately, we were not able to obtain a single crystal of the anhydrous compound. Anyhow, the previously described single crystal structure of monohydrate have been found very useful, and comparisons of FT-IR spectrum and thermal behavior of the anhydrous and monohydrated forms have definitely confirmed differences in degree of hydration and solid state structure, while those of ^{1}H- and ^{13}C-NMR spectra proved the molecular identity of the two forms. The achieved indexing - confirmed by the unit cell content modelling - may enrich the 'low precision' reference powder XRD card information (PDF 00-021-1604) of the anhydrous title compound in the PDF database, as well.

Acknowledgements

References

[1] Allen, F. H. "The Cambridge Structural Database: a quarter of a million crystal structures and rising", Acta Crystallographica Section B, B58, pp. 380–388, 2002.
https://doi.org/10.1107/S0108768102003890

[2] Szokol, Z., Lozsi, K., Virág, A., Dancsó, A., Szlávik, L., Simig, G., Volk, B. "Assignment of Absolute Configuration to Enantiomers of Anti-Alzheimer Drug Candidate Blarcamesine", Periodica Polytechnica Chemical Engineering, 66(4), pp. 536–540, 2022.
https://doi.org/10.3311/PPch.20662

[3] David, W. I. F., Shankland, K. "Structure determination from powder diffraction data", Acta Crystallographica Section A, A64, pp. 52–64, 2008.
https://doi.org/10.1107/S0108767307064252

[4] Shankland, K., Spillman, M. J., Kabova, E. A., Edgeley, D. S., Shankland, N. "The principles underlying the use of powder diffraction data in solving pharmaceutical crystal structures", Acta Crystallographica Part C, C69, pp. 1251–1259, 2013.
https://doi.org/10.1107/S0108270113028643

[5] Spillman, M. J., Shankland, K. "GALLOP: accelerated molecular crystal structure determination from powder diffraction data", CrystEngComm, 37(23), pp. 6481–6485, 2021.
https://doi.org/10.1039/d1ce00978h

[6] David, W. I. F., Shankland, K., van de Streek, J., Pidcock, E., Motherwell, W. D. S., Cole, J. C. "DASH: A program for crystal structure determination from powder diffraction data", Journal of Applied Crystallography, 39, pp. 910–915, 2006.
https://doi.org/10.1107/S0021889806042117

[7] Cambridge Crystallographic Data Centre (CCDC) "Crystal Structure Database (CSD), (v.5.43)", Available at: https://www.ccdc.cam.ac.uk/solutions/csd-core/components/csd/ [Accessed: 06 July 2023]

[8] Kabova, E. A., Cole, J. C., Korb, O., López-Ibáñez, M., Williams, A. C., Shankland, K. "Improved performance of crystal structure solution from powder diffraction data through parameter tuning of a simulated annealing algorithm", Journal of Applied Crystallography, 50, pp. 1411–1420, 2017.
https://doi.org/10.1107/S1600576717012602

[9] Kabova, E. A., Cole, J. C., Korb, O., Williams, A. C., Shankland, K. "Improved crystal structure solution from powder diffraction data by the use of conformational information", Journal of Applied Crystallography, 50, pp. 1421–1427, 2017.
https://doi.org/10.1107/S1600576717012596

[10] Ávila, E. E., Mora, A. J., Delgado, G. E., Contreras, R. R., Rincón, L., Fitch, A. N., Brunelli, M. "Structure and conformational analysis of a bidentate pro-ligand, $C_{21}H_{34}N_2S_2$, from powder synchrotron diffraction data and solid-state DFTB calculations", Acta Crystallographica Section B, B65, pp. 639–646, 2009.
https://doi.org/10.1107/S0108768109027244

[11] Ferreira, F. F., Antonio, S. G., Rosa, P. C. P., Paiva-Santos, C. O. "Crystal Structure Determination of Mebendazole Form A Using High-Resolution Synchrotron X-Ray Powder Diffraction Data", Journal of Pharmaceutical Sciences, 99(4), pp. 1734–1744, 2010.
https://doi.org/10.1002/jps.21902

[12] Florence, A. J., Shankland, N., Shankland, K., David, W. I. F., Pidcock, E., Xu, X., Johnston, A., Kennedy, A. R., Cox, P. J., Evans, J. S. O., Steele, G., Cosgrove, S. D., Frampton, C. S. "Solving molecular crystal structures from laboratory X-ray powder diffraction data with DASH: the state of the art and challenges", Journal of Applied Crystallography, 38, pp. 249–259, 2005.
https://doi.org/10.1107/S0021889804032662

[13] van de Streek, J., Brüning, J., Ivashevskaya, S. N., Ermrich, M., Paulus, E. F., Bolte, M., Schmidt, M. U. "Structures of six industrial benzimidazolone pigments from laboratory powder diffraction data", Acta Crystallographica Section B, B65, pp. 200–211, 2009.
https://doi.org/10.1107/S0108768108041529

[14] Ivashevskaya, S. N., van de Streek, J., Djanhan, J. E., Brüning, J., Alig, E., Bolte, M., Schmidt, M. U., Blaschka, P., Höffken, H. W., Erk, P. "Structure determination of seven phases and solvates of Pigment Yellow 183 and Pigment Yellow 191 from X-ray powder and single-crystal data", Acta Crystallographica Section B, B65, pp. 212–222, 2009.
https://doi.org/10.1107/S0108768109001827

[15] Toro, R. A., Dugarte-Dugarte, A., van de Streek, J., Henao, J. A., Delgado, J. M., de Delgado, G. D. "Crystal structure from X-ray powder diffraction data, DFT-D calculation, Hirshfeld surface analysis, and energy frameworks of (RS)-trichlormethiazide", Acta Crystallographica Section E, E78, pp. 140–148, 2022.
https://doi.org/10.1107/S2056989021013633

[16] Brüning, J., Alig, E., Schmidt, M. U. "Ezetimibe anhydrate, determined from laboratory powder diffraction data", Acta Crystallographica Section C, C66, pp. o341–o344, 2010.

[17] Guguta, C., Peters, T. P. J., de Gelder, R. "Structural Investigations of Hydrate, Anhydrate, Free Base, and Hydrochloride Forms of Morphine and Naloxone", Crystal Growth & Design, 8(11), pp. 4150–4158, 2008.
https://doi.org/10.1021/cg800622m

[18] Guguta, C., van Eck, E. R. H., de Gelder, R. "Structural Insight into the Dehydration and Hydration Behavior of Naltrexone and Naloxone Hydrochloride. Dehydration-Induced Expansion versus Contraction", Crystal Growth & Design, 9(8), pp. 3384–3395, 2009.
https://doi.org/10.1021/cg801051u

[19] Hayriye, A. "Bisantipyrylmethane [1251—85-0]", Reviews of Faculté Science, University of Istanbul, 14A(2), pp. 90–97, 1949. [online] Available at: https://www.chemblink.com/products/1251-85-0.html [Accessed: 22 December 2022]

[20] Passerini, M. "Reactions of hexamethylenetetramine I", Gazzetta Chimica Italiana, 89, pp. 1645–1653, 1959.

[21] Kaufmann, H. P. "Synthetical studies on pharmaceutical products. XVI. Antipyryl ketones", Berichte der Deutschen Chemischen Gesellschaft [Abteilung] B: Abhandlungen, 75B, pp. 1236–1247, 1942.

[22] Sciortino, T. "Cyclamates of pharmaceutical interest. I. Cyclamates of pyrazolone drugs", Bollettino Chimico Farmaceutico, 104(5), pp. 292–299, 1965.

[23] Ito, I., Ueda, T., Kurokawa, E. "Synthesis of Pyrazolone Derivatives. X. Synthesis of 2, 4, 6-Trioxohexahydro-5-pyrimidinyl Derivatives", Chemical and Pharmaceutical Bulletin, 14(3), pp. 207–211, 1966.
https://doi.org/10.1248/cpb.14.207

[24] Hellmann, H., Opitz, G. "Beiträge zum Mechanismus der Aminomethylierungsreaktion V. Sulfinsäuren in der Aminoalkylierungsreaktion" (Contributions to mechanism of the aminomethylating reaction, V. Sulfinic acids in the aminomethylating reaction), Chemische Berichte, 90(1), pp. 8–14, 1957. (in German)
https://doi.org/10.1002/cber.19570900103

[25] Lieberman, S. V., Wagner, E. C. "The course of the Mannich reaction", The Journal of Organic Chemistry, 14(6), pp. 1001–1012, 1949.
https://doi.org/10.1021/jo01158a008

[26] Merz, K. "4,4'-Methylenediantipyrine monohydrate", Acta Crystallographica Section E, E58, pp. o338–o340, 2002.
https://doi.org/10.1107/S1600536802003331

[27] Akhmadiev, N. S., Mescheryakova, E. S., Akhmetova, V. R. Khairullina, V. R. Khalilov, L. M. Ibragimov, A. G. "Synthesis, Crystal Structure and Docking Studies as Potential Anti-Inflammatory Agents of Novel Antipyrine Sulfanyl Derivatives", Journal of Molecular Structure, 1228, 129734, 2021.
https://doi.org/10.1016/j.molstruc.2020.129734

[28] International Centre for Diffraction Data (ICDD) "Powder Diffraction File, PDF-4+, Release 2022", [academically subscribed, publically not available] Homepage at: https://www.icdd.com/ [Accessed: 22 December 2022]

[29] Boultif, A., Louer, D. "Indexing of powder diffraction patterns for low-symmetry lattices by the successive dichotomy method", Journal of Applied Crystallography, 24, pp. 987–993, 1991.
https://doi.org/10.1107/S0021889891006441

[30] Markvardsen, A. J., David, W. I. F., Johnson, J. C., Shankland, K. "A probabilistic approach to space-group determination from powder diffraction data", Acta Crystallographica Section A, A57, pp. 47–54, 2001.
https://doi.org/10.1107/S0108767300012174

[31] National Institute of Advanced Industrial Science and Technology (AIST) "Spectral Database for Organic Compounds, SDBS", [online] Available at https://sdbs.db.aist.go.jp/sdbs/cgi-bin/cre_index.cgi [Accessed: 22 December 2022]

[32] American Chemical Society "SciFindern", [online] Available at: https://scifinder-n.cas.org/ [Accessed: 30 November 2022]

[33] Saeed, A., Khurshid, A., Flörke, U., Echeverría, G. A., Piro, O. E., Gil, D. M., Rocha, M., Frontera, A., El-Seedi, H. R., Mumtaz, A., Erben, M. F. "Intermolecular interactions in antipyrine-like derivatives 2-halo-N-(1,5-dimethyl-3-oxo-2-phenyl-2,3-dihydro-1H-pyrazol-4-yl)benzamides: X-ray structure, Hirshfeld surface analysis and DFT calculations", New Journal of Chemistry, 45(44), pp. 19541–19554, 2020.
https://doi.org/10.1039/D0NJ03958F

[34] Lévay, K., Madarász, J., Hegedűs, L. "Tuning the chemoselectivity of the Pd-catalysed hydrogenation of pyridinecarbonitriles: an efficient and simple method for preparing pyridyl- or piperidylmethylamines", Catalysis Science & Technology, 8(12), pp. 2634–2648, 2022.
https://doi.org/10.1039/d1cy02295d

[35] Kabova, E. A., Blundell, C. D., Shankland, K. "Pushing the limits of molecular crystal structure determination from powder diffraction data in high-throughput chemical environments", Journal of Pharmaceutical Sciences, 107(89), pp. 2042–2047, 2018.
https://doi.org/10.1016/j.xphs.2018.04.010